Effect of Airborne Particle Abrasion Protocols on the Shear Bond Strength and Surface Hardness of High-Translucent Zirconia Under Thermocycling: An In-Vitro Study

Reem Mohsen AlMutairi *

Posted Date: 6 October 2025

doi: 10.20944/preprints202510.0378.v1

Keywords: zirconium; dental porcelain; surface properties; shear strength; hardness tests; dental bonding

 doi:10.20944/preprints202510.0378.v1

Article

Effect of Airborne Particle Abrasion Protocols on the Shear Bond Strength and Surface Hardness of High-Translucent Zirconia Under Thermocycling: An In-Vitro Study

Reem Mohsen AlMutairi

Department of Restorative Dental Sciences and Prosthodontics, College of Dentistry, Majmaah University, Al-Majmaah 11952, Saudi Arabia; reem.m@mu.edu.sa

Abstract

High-translucent 5Y-PSZ zirconia offers superior esthetics but reduced mechanical strength, complicating resin–zirconia bonding and durability under thermocycling. This in vitro study evaluated the effect of airborne-particle abrasion (APA) protocols on the shear bond strength (SBS) and surface hardness (SH) of high-translucent zirconia (Shofu ZR Lucent) under thermocycling. Thirty CAD-CAM specimens were divided into three groups (n = 10) based on the APA protocol: control, 50 μm Al_2O_3, and 100 μm glass microbeads. Fifteen square specimens (n= 5 per group with dimensions 8 × 8 × 3 mm) were bonded with primer (AZ Primer) and resin cement (ResiCem) for SBS testing, and fifteen discs (n= 5 per group with dimensions 15 × 1.2 mm) were used for SH evaluation. All samples underwent 25,000 thermocycles between 5-55 °C. SBS values did not differ significantly among groups (control: 5.64 ± 1.49 MPa; 50 μm Al_2O_3: 6.49 ± 1.59 MPa; 100 μm glass microbeads: 6.42 ± 4.05 MPa; ANOVA $p = 0.852$), with 100% adhesive failures at the resin–zirconia interface. In contrast, SH differed markedly (control: 876.34 ± 25.10 VHN; 50 μm Al_2O_3: 1747.26 ± 37.37 VHN; 100 μm glass microbeads: 1246.94 ± 33.81 VHN; ANOVA $p < 0.001$), with all pairwise comparisons significant (Tukey $p < 0.001$). These findings indicate that while APA does not improve SBS, but it substantially enhances surface hardness, particularly with 50 μm Al_2O_3, which may strengthen the zirconia surface and improve long-term wear resistance.

Keywords: zirconium; dental porcelain; surface properties; shear strength; hardness tests; dental bonding

1. Introduction

Zirconia, which is a crystalline form of zirconium oxide (ZrO2), has become a material of choice in restorative dentistry and prosthodontics because of its superior mechanical strength, favorable optical properties and excellent biocompatibility [1,2]. The increasing demand for metal-free, esthetically pleasing restorations and advances in computer-aided design and computer-aided manufacturing (CAD-CAM) technologies have driven the development of zirconia systems with tailored translucency, optimized strength and improved machinability [3,4].

Structurally, zirconia exists in three crystallographic phases with distinct clinical implications. The monoclinic phase is stable at room temperature upto 1170 °C but brittle; the tetragonal phase (stable between 1170 °C and 2370 °C) confers transformation toughening and high fracture toughness; and the cubic phase (stable above 2370 °C) yields high translucency but reduced mechanical strength [5–8]. Stabilization with yttria (yttrium oxide Y_2O_3) retains tetragonal or cubic phases at room temperature and thereby governs the trade-off between optical and mechanical behavior critical for dental applications [6,7].

 doi:10.20944/preprints202510.0378.v1

The generational evolution of dental zirconia reflects efforts to balance strength and esthetics. First-generation 3 mol% yttria-stabilized tetragonal zirconia polycrystal (3Y-TZP), introduced as "white metal", contained approximately 0.25 wt% alumina (aluminium oxide Al_2O_3) and was composed almost entirely of the tetragonal phase. While offering high strength and fracture toughness, its opacity which was driven by light scattering at grain boundaries, inclusions and porosities, limited its use to frameworks and porcelain-layered crowns [8,9]. Second-generation 3Y-TZP reduced alumina content and employed higher sintering temperatures to lower porosity and improve translucency, yet esthetics remained insufficient for monolithic anterior restorations [8,9]. Subsequent fourth-generation 4 mol% yttria-partially stabilized zirconia (4Y-PSZ) and third-generation 5 mol% yttria-partially stabilized zirconia (5Y-PSZ) materials increased cubic-phase content to deliver enhanced translucency and optical mimicry. However, this improvement was accompanied by diminished transformation toughening and reduced fracture resistance [10,11]. Ban further classified yttria-stabilized zirconia into 12 categories based on yttria concentration, chromatic uniformity, compositional homogeneity and layering, underscoring the persistent challenge of balancing translucency with mechanical reliability [12].

High-translucent 5Y-PSZ (vernacular name "cubic" zirconia) markedly improves optical properties but does so at the expense of mechanical strength [12–18]. These materials typically exhibit a cubic-tetragonal microstructure with greater than 50% cubic phase and are more translucent because their isotropic crystallography reduces light scattering at grain boundaries [19,20]. Increased yttria reduces tetragonality ratio of remaining tetragonal grains, and some grains become "non-transformable," which diminishes transformation toughening and contributes to lower fracture resistance [21–23]. Although high-translucent yttria 5Y-PSZ is less susceptible to low temperature degradation (LTD), when it occurs, can still reduce shear bond strength and surface hardness and increase surface roughness [24–27].

The absence of silica and a glass phase in zirconia renders hydrofluoric acid etching and silane coupling ineffective, necessitating alternative surface treatment strategies to achieve durable bonding with resin cements [28,29]. Surface treatments for zirconia can be broadly classified into mechanical, chemical, or hybrid approaches. Mechanical methods include airborne particle abrasion (APA) using Al_2O_3 particles [30], tribo-chemical silica coating [31], grinding [32], polishing [33], and various laser irradiations [34–36]. Other mechanical techniques include selective infiltration etching [37], plasma spraying [38] or non-thermal plasma etching, including argon plasma with or without surface abrasion [39], ceramic or glaze coatings using low-fusion porcelain [40], zirconia or alumina particle coatings, including nano-structured alumina [41] and alumina via aluminum nitride suspension [42], and hot chemical etching solutions [43–45]. Experimental approaches, such as bioglass particle abrasion [46] and slurry silica coating [47] have also been reported. Specialized techniques include zirconia surface architecturing technique (ZSAT), which employs a mixed nitric and hydrofluoric acid solution [48] and commercial etching solutions such as zircos-E, hydrofluoric acid, hydrochloric acid, and Ferric chloride [20]. Chemical methods include primers containing functional monomers such as 10-methacryloyloxydecyl dihydrogen phosphate (10-MDP) [49,50] and silane coupling agents [28], immersion in chemical solutions including silicon nitride [51], silicon nitride treated with sodium hydroxide [51], 37% phosphoric acid [52], piranha solution (sulfuric acid and hydrogen peroxide in 3:1 ratio) [53], and hot hydrochloric acid etching [54], plasma treatments [38,39] and silica-based epitaxial transition film formation [55]. Hybrid approaches involve integrating mechanical and chemical methods have also been proposed in literature [56,57]. Despite the diversity of methods, no single surface treatment has been shown to ensure consistently optimal bonding for zirconia restorations [28,29]. However, these treatments aim to optimize micromechanical interlocking and/or chemical adhesion while preserving mechanical integrity [58]. Many surface treatments alter not only alter microroughness and chemical reactivity but also shear bond strength (SBS) and surface hardness (SH)- these properties influence the resistance to surface damage, antagonist wear, fatigue performance and the stability of the adhesive interface [59,60].

 doi:10.20944/preprints202510.0378.v1

The "APC Zirconia Bonding Concept" described by Blatz et al. [61], is the widely adopted surface treatment method, consisting of three steps: APA (step A) to create a rough surface, applying a ceramic primer containing adhesive phosphate monomers (step P), and bonding with dual- or self-cure composites (step C). Some studies also report that APA with 50-μm Al_2O_3 combined with 10-MDP chemistry (MDP-containing primer or cement) maximizes SBS while better preserving surface integrity [62,63]. Alternative, less-aggressive blasting media such as glass beads have been proposed for high-translucent zirconia to reduce iatrogenic damage. Glass-bead abrasion is commonly used on enamel, dentin and nickel-chromium (Ni-Cr) alloys, but typically yields lower bond strengths for Ni-Cr compared with alumina and can reduce adhesion to enamel and dentin [63,64]. Because glass beads are softer than alumina, they may preserve SH in high-translucent zirconia [65]. Few research reported that APA with alumina abrasion impaired flexural strength of zirconia more than glass-bead abrasion, supporting material-specific choices of blasting media [65,66]. The variable parameters in APA with alumina are grain size (25 to 250 μm), propulsion pressure (0.05 to 0.45 MPa), distance (5 to 20 mm) from the nozzle to the specimen, and time of APA (5 to 30 seconds) [67]. Particle size can critically influence outcomes: controlled roughening (50 μm) is generally favorable, whereas larger particles (110- 250 μm) may induce microcracks and surface flaws that reduce fracture resistance and can also decrease SH [67–70]. However, the evidence about the effects of low-abrasive particles on SH and SBS for high-translucent zirconia remains limited.

Aging simulations, such as thermocycling, can reduce zirconia's SBS and SH, making initial measurements alone unreliable for predicting long-term performance. Combining SBS and SH assessments under artificial aging better evaluates a surface treatment's clinical suitability, reflecting adhesive integrity, hardness retention, and failure mode patterns [58].

To address these gaps, this in-vitro study was designed to evaluate the effect of APA protocols on the SBS and SH of high-translucent zirconia under thermocycling. The null hypotheses (H_0) as follows: (1) There is no significant difference in the SBS of high-translucent zirconia treated with 50-μm Al_2O_3 or 100-μm glass microbead APA under thermocycling; (2) There is no significant difference in the SH of high-translucent zirconia treated with 50-μm Al_2O_3 or 100-μm glass microbead APA under thermocycling. The alternative hypotheses (Ha) as follows: (1) Air abrasion with 50-μm Al_2O_3 or 100-μm glass microbeads significantly alters the SBS of high-translucent zirconia under thermocycling; (2) Air abrasion with 50-μm Al_2O_3 or 100-μm glass microbeads significantly alters the SH of high-translucent zirconia under thermocycling.

2. Materials and Methods

The detailed specifications of the materials used in this study are summarized in Table 1.

Table 1. Materials used in this study.

Material	Brand and Manufacturer	Shade and Composition
High- Translucent 5Y-PSZ Zirconia Ceramic	ZR Lucent, Shofu Dental Corporation, Kyoto, Japan	Shade: A2; Composition: A multilayer zirconia disc with dimensions 98.5 × 18 mm fabricated from 100% Tosoh zirconia powder, containing 5 mol% yttria-stabilized zirconia (5Y-PSZ). The disc comprises five gradient layers with varying translucency and strength: one enamel layer (30%), three dentin layers (35%), and one cervical layer (35%). Exact oxide weight percentages are not disclosed in

 doi:10.20944/preprints202510.0378.v1

		the manufacturer's literature [71].
Dual cure adhesive resin cement	ResiCem, Shofu Dental Corporation, Kyoto, Japan	Shade: Clear; Composition: Paste A- UDMA, TEGDMA, Fluoro-alumino-silicate glass, initiator [75]. Paste B- UDMA, TEGDMA, Carboxylic acid monomer, 4-AET, 2-HEMA, Fluoro-alumino-silicate glass, initiator [75].
Primer	AZ primer, Shofu Dental Corporation, Kyoto, Japan	Composition: Phosphonic acid monomer (6-MHPA), Thioctic acid monomer, Acetone [74].
50-μm Al_2O_3	Korox 50, Bego, Germany	Composition: 99.6 % Al_2O_3, special corundum, other constituents [72].
100-μm glass microbeads	Rolloblast, Renfert, Germany	Composition: Glass microbeads [73].

2.1. Test Material (Manufacturer Data) [71]

Shofu ZR Lucent (Shofu Dental Corporation, Kyoto, Japan) is a polychromic, multilayered 5Y-PSZ disk marketed to synchronize strength and esthetics. According to the manufacturer, it is produced from high-quality Tosoh zirconia powder and exhibits a five-layer graded design (approximate enamel/dentin/cervical distribution reported as 30%/35%/35% respectively) with a uniform flexural strength of approximately 1019 MPa across the gradient and translucency values ranging from approximately 31–37% (comparable to lithium disilicate) with reported improved masking of discolored substrates. Manufacturer data also report Vickers hardness 45 HV (unsintered), coefficient of thermal expansion 10.2×10^{-6} K^{-1} and sintering temperature 1450 °C; the material is intended for anterior and posterior crowns, short-span bridges, veneers, inlays and onlays with options for staining/micro-layering. The data presented are manufacturer-reported specifications [71]; independent, peer-reviewed thermocycling data on SH and SBS for Shofu ZR Lucent are currently limited or unavailable, which motivates the present investigation.

2.2. Experimental Workflow

The experimental workflow of the study is summarized in Figure 1.

 doi:10.20944/preprints202510.0378.v1

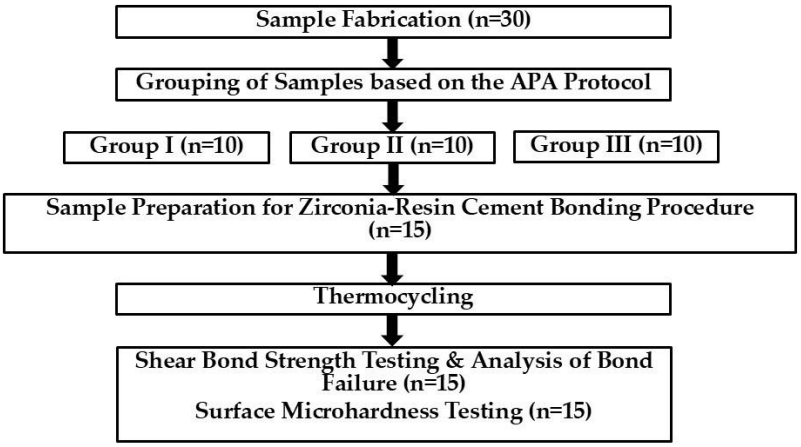

Figure 1. Experimental workflow.

2.3. Sample Fabrication

Thirty samples were fabricated from pre-sintered high-translucent zirconia blocks (Shofu ZR-Lucent, Japan) using subtractive CAD-CAM technology (Imes icore 350i, Germany). Fifteen square samples with dimensions 8 × 8 × 3 mm were allocated for SBS testing (Figure 2a), and fifteen disc-shaped samples with dimensions 15 × 1.2 mm were used for SH evaluation (Figure 2b).

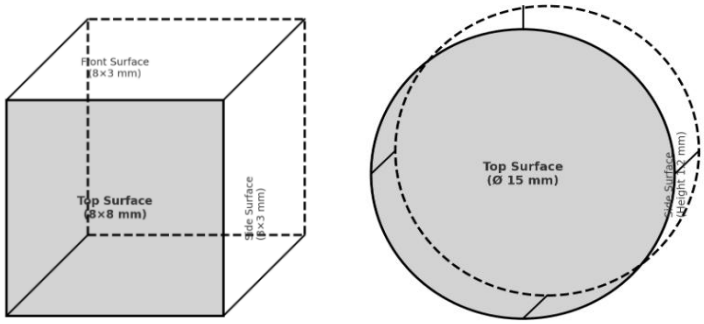

(**a**) (**b**)

Figure 2. Schematic illustration of zirconia sample dimensions. (**a**) square-shaped specimen; (**b**) disc- shaped specimen.

Samples were sintered in a furnace (S-600; Add-in Co., Ltd., Goyang, Korea) at 1450 °C for 120 minutes with a heating and cooling rate of 5–10 °C/min following the manufacturer's instructions. Surfaces were sequentially polished to minimize surface defects under wet conditions with 600-, 1000- and 1200-grit silicon carbide paper (15 seconds per grit) The samples were then ultrasonicated (GT Ultrasonic Co. Ltd., China) in distilled water for 10 minutes, and air-dried.

2.4. Grouping of Samples based on the APA Protocol

Samples were randomly divided into three groups (n = 10) based on the APA protocol:

Group I (Control): No air abrasion.

Group II: Air abrasion with 50 μm Al_2O_3 (Korox 50, Bego, Germany) [72] for 20 seconds at 2 bar pressure in a sandblaster (BEGO Easy Blast sandblaster, Germany), with the nozzle positioned at 90º to the center of the sample at 10 mm distance.

Group III: Air abrasion with 100 μm glass microbeads (Rolloblast, Renfert, Germany) [73] under identical conditions.

 doi:10.20944/preprints202510.0378.v1

After air abrasion, all samples were cleaned with an air syringe and ultrasonicated in distilled water for 10 minutes.

2.5. Sample Preparation for Zirconia-Resin Cement Bonding Procedure

The samples were ultrasonically cleaned with 99% isopropanol for 180 seconds, and air-dried. Each square sample was embedded in one mm self-curing acrylic resin (Takilon, Rodent s.r.l., Milan, Italy) block. To define the bonding area, silicon molds with 2 mm diameter and 2 mm length were fabricated and positioned on the center of the zirconia samples [63] to create a standardized bonding area of 12.25 mm2. A manufacturer-recommended zirconia primer (AZ Primer, Shofu Inc., Kyoto, Japan) [74] was applied to the designated bonding surface, followed by dual-cure resin cement (ResiCem, Shofu, Kyoto, Japan) [75]. The primer was applied to the designated zirconia bonding surface using a disposable microbrush applicator and left undisturbed for 10 seconds. The resin cement was applied directly on the fabricated silicon molds and excess cement was removed using a microbrush. Chemical curing was initiated 30 seconds after primer application and allowed to proceed for 3 minutes. Light cure polymerization was performed for 40 seconds (10 seconds per side) using a light-emitting diode unit (Bluephase, Ivoclar Vivadent, Schaan, Liechtenstein) with an intensity of 1400 mW/cm2. The bonded samples (Figure 3) were stored in distilled water for 7 days at 37 °C prior to thermocycling to allow post-cure polymerization and initial stabilization of the mechanical properties of the resin cement. A 7-day baseline period, consistent with prior research [76], was employed in this study.

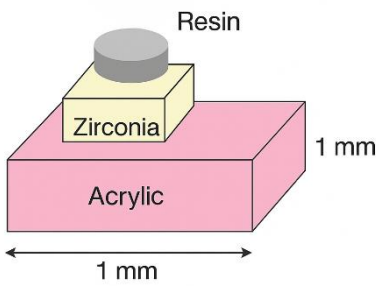

Figure 3. Schematic illustration of the zirconia–resin cement bonded specimen.

2.6. Thermocycling

Artificial aging was simulated by 25,000 thermocycles in two thermostatic water baths (water-to-water transfer) ranging from 5- 55°C using a thermocycler (Haake Circulating Bath DC-15 with Haake DC 10 Thermocontroller, Thermo Haake, USA) in all the samples. Each cycle lasted for 30 seconds and involved the following steps: 10 seconds in a 5°C bath, 5 seconds for transfer, 10 seconds in a 55°C bath, and 5 seconds for returning to the 5°C bath. The chosen temperature range and dwell times follow common laboratory practice (ISO 10477, 1996; ISO 4049:2009; ISO 29022:2013) and the 25,000-cycle regimen was selected to simulate extended clinical aging (approximately 2.5 years of intraoral use based on Gale & Darvell [77] and to exceed the frequently used 10,000-cycle (approximately 1 year) threshold discussed in the literature [58,77]. After thermocycling, the samples were rinsed and dried.

2.7. Shear Bond Strength Testing and Analysis of Bond Failure

SBS testing was performed on the bonded square samples (n= 5 per group) using a universal testing machine (Instron 3345, UK) according to ISO TR11405. Each bonded specimen was mounted in the testing jig of the universal testing machine. A knife-edge shear test was performed using a with a 5 kN load cell and a crosshead speed of 0.5 mm/min, and the shear load at failure (N) was recorded. The knife edge was positioned at the interface between the zirconia and the resin cement to induce

 doi:10.20944/preprints202510.0378.v1

bond failure. SBS (MPa) values were converted from Newtons to megapascals (MPa) (1 N/mm² = 1 MPa) and then calculated by dividing the load at failure (N) by the standardized interfacial area (12.25 mm²) [63].

Shear bond strength (MPa)= Failure load (N)/ Surface area (mm²)

Debonded samples were examined under a stereomicroscope (Nikon SMZ25 stereo microscope, Japan) at 40X magnification. Failure modes were recorded as classified by Serra-Prat et al. [78] as follows:

Type I- cohesive (failure within the cement, when approximately two-thirds or more of the luting agent remained on the zirconia surface).

Type II- adhesive (failure at the cement–zirconia interface, when less than one-third of the cement remained).

Type III- mixed (combined adhesive and cohesive features, when approximately one-third to two-thirds of the cement remained or both interfacial and bulk fractures were observed).

2.8. Surface Microhardness Testing

Microhardness testing was performed on disc-shaped samples (n= 5 per group) using a Vickers microhardness tester (Buehler, Lake Bluff, IL, USA) according to ISO 6507-1. A square-based pyramidal diamond indenter was applied at a constant load of 10 N for 10 s. Three indentations were made randomly on each specimen, and the mean value was calculated. The two diagonals (D1, D2) of each indentation were measured using digital microscopy (KH-7700, Hirox, Tokyo, Japan), and their average length (L) was used for calculation [21]. The Vickers hardness number (VHN) was determined using the formula [79]:

Surface Hardness (VHN) =1.854 P/ L2

where P is the applied load (kgf) and L=(D1+D2)/2 is the mean diagonal length in mm.

2.9. Statistical Analysis

Statistical analyses were performed using IBM SPSS Statistics, version 30 (IBM Corp., Armonk, NY, USA). Data normality was assessed using the Shapiro–Wilk test ($p > 0.05$). One-way ANOVA evaluated the effect of surface treatment on SBS and SH, followed by Tukey's post-hoc test for pairwise comparisons. Homogeneity of variances was confirmed using Levene's test. Statistical significance was set at $p \leq 0.05$, and results are presented as mean ± standard deviation.

3. Results

3.1. Shear Bond Strength

The mean SBS values for control, 50 µm Al_2O_3, and 100 µm glass microbead groups were 5.64 ± 1.49 MPa, 6.49 ± 1.59 MPa, and 6.42 ± 4.05 MPa, respectively (Table 2).

Table 2. Shear bond strength of high-translucent zirconia under thermocycling.

Group	Mean (MPa) ± SD	Mean Difference (MPa)	P value
I- Control	5.64 ± 1.49	-	-
II- 50 µm Al_2O_3	6.49 ± 1.59	vs I: 0.85	vs I: 0.875
III- 100 µm Glass Microbeads	6.42 ± 4.05	vs I: 0.78 vs II: - 0.07	vs I: 0.889 vs II: 0.999

Data were normally distributed (Shapiro–Wilk, $p > 0.05$). One-way ANOVA revealed no significant difference in SBS among groups ($F(2,12) = 0.162$, $p = 0.852$). Post-hoc Tukey tests confirmed no pairwise differences ($p > 0.05$), with mean differences of 0.85 MPa (50 µm Al_2O_3 vs control),

 doi:10.20944/preprints202510.0378.v1

0.78 MPa (100 µm glass microbeads vs control), and −0.07 MPa (100 µm glass microbeads vs 50 µm Al_2O_3). All failures (100%) were adhesive at the zirconia–resin interface (Figure 4).

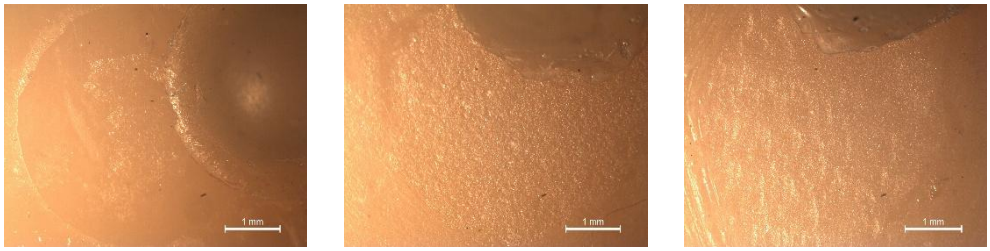

(**a**) (**b**) (c)

Figure 4. Representative stereomicroscopic images at 40X magnification showing adhesive failure at the zirconia–resin interface: (**a**) control; (**b**) 50 µm Al_2O_3; (**c**) 100 µm glass microbeads.

3.2. Surface Hardness

Vickers microhardness values differed significantly among groups ($F(2,12) = 903.83$, $p < 0.001$). The mean SH was lowest in the control group (876.34 ± 25.10 VHN), followed by 100 µm glass microbeads (1246.94 ± 33.81 VHN) and 50 µm Al_2O_3 (1747.26 ± 37.37 VHN) (Table 3).

Table 3. Surface hardness of high-translucent zirconia under thermocycling

Group	Mean (MPa) ± SD	Mean Difference (MPa)	P value
I- Control	876.34 ± 25.10	-	-
II- 50 µm Al_2O_3	1747.26 ± 37.37	vs I: 870.92	vs I: < 0.001*
III- 100 µm Glass Microbeads	1246.94 ± 33.81	vs I: 370.60 vs II: - 500.32	vs I: < 0.001* vs II: < 0.001*

* Statistically significant at $P \leq 0.05$.

Post-hoc Tukey tests revealed all pairwise differences were statistically significant ($p < 0.001$), with mean differences of 370.60 VHN (100 µm glass microbeads vs control), 870.92 VHN (50 µm Al_2O_3 vs control), and −500.32 VHN (50 µm Al_2O_3 vs 100 µm glass microbeads). The digital microscopy images reveal the brittle nature of the tested material (Figure 5).

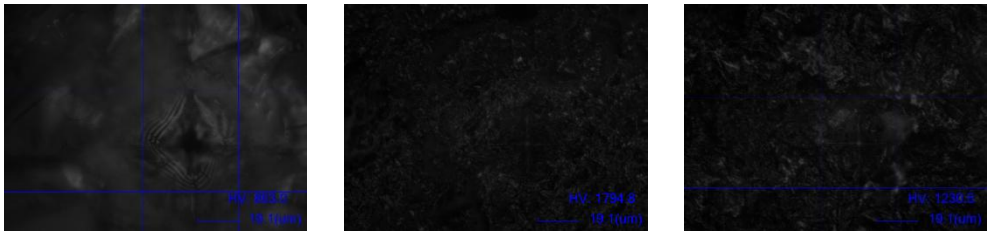

(**a**) (**b**) (c)

Figure 5. Representative digital microscopy images showing Vickers indentations and microcrack patterns on zirconia surfaces: (**a**) control; (**b**) 50 µm Al_2O_3; (**c**) 100 µm glass microbeads.

4. Discussion

APA protocols exert distinct and sometimes opposing effects on bond strength and surface hardness in high-translucent zirconia. The null hypothesis (H_0) was accepted in the study as there was no significant difference in the SBS of high-translucent zirconia treated with 50-µm Al_2O_3 or 100-µm glass microbead APA under thermocycling. These results align with prior reports showing that increased surface roughness from APA does not inevitably produce durable bond gains and that

 doi:10.20944/preprints202510.0378.v1

thermal ageing often unmasks interfacial weakness [80–82]. Similarly, some studies report minimal or no SBS gain after APA for certain ultra-translucent or high-cubic zirconia [27,60,63,66,83]. In fact, a few studies have documented reduced bulk strength after aggressive APA. These effects may result from altered tetragonal→monoclinic (t→m) transformation dynamics, increased cubic content, or surface flaws introduced during blasting [83,84].

Mechanistically, these divergent outcomes can be explained by the impact physics of different abrasives and the chemistry of contemporary high-translucent zirconia. Angular, hard Al_2O_3 particles induce localized plastic deformation and a peening effect, referring to the localized hammering action of abrasive particles, which compacts the surface. This densifies the outermost microns and can trigger a thin t→m surface transformation [30,68,85]. By contrast, spherical glass microbeads are less aggressive, generating milder topographical changes while preserving subsurface integrity [63,86].

Importantly, increased topographical roughness alone does not guarantee improved micromechanical retention. Resin penetration into micro-retentions, wetting behavior, and the integrity of the chemically bonded interface ultimately determine durable SBS [70,87]. Tzanakakis and colleagues emphasized that grain size, pressure, and exposure time produce variable roughness but do not reliably predict long-term SBS [82]. Aggressive blasting can increase monoclinic content and microcracking, undermining mechanical performance [82].

Adhesive bond failures in the control groups align with expectations, as untreated zirconia is chemically inert, has low surface energy, and limited micromechanical retention. Consequently, unconditioned zirconia often debond at the cement–ceramic interface, particularly after aging [88,89]. In the present study, APA-treated groups also exhibited exclusively adhesive failures. This contrasts with previous literature reporting predominantly mixed or cohesive failures [49,86,90]. Non-adhesive failures are indirect markers of stronger interfacial adhesion because surface roughening increases contact area and promotes resin penetration. Mehari et al. and others reported a shift toward mixed/cohesive failures with Al_2O_3 APA compared with glass-bead or untreated surfaces, which disagrees with the present observations [86]. The adhesive failures observed here could be attributed to the thermocycling procedure. Cyclic thermal shocks and associated water sorption accelerate hydrolytic degradation of the adhesive interface, reliably reducing resin-zirconia bond strength compared with immediate values [81,91]. Thermocycling thus provides a more stringent evaluation of APA protocols and adhesive strategies. Other studies similarly report adhesive bond failures after ageing, despite initial increases in immediate SBS [92,93].

These findings align with multiple laboratory reports showing that Al_2O_3 APA increases surface roughness and mechanical interlocking, producing higher immediate SBS values compared with glass beads or untreated surfaces [86,94]. The benefit of APA is often amplified when combined with chemical coupling. Clinically, the adhesive failures and non-significant SBS differences observed here underscore the need to pair mechanical conditioning with robust chemical bonding protocols to optimize outcomes. Previous literature suggests that APA benefits are magnified when combined with MDP-containing primers or cement chemistry that promotes durable chemical bonding, resulting in higher SBS and often mixed/cohesive failure modes [50,58,81,87,95–97].

From a practical perspective, modest APA using 50-μm Al_2O_3 at controlled pressure, followed by an MDP-containing primer or cement, provides a reliable pathway to durable bonding for many zirconia types [58,70,96]. Where conservation of core strength is critical (e.g., thin sections, highly cubic 5Y-PSZ), less aggressive protocols-using finer particles, lower pressure or alternative surface treatments such as tribochemical silica coating and optimized primers may offer a better balance between bondability and structural integrity [51,86,94].

Hardness represents resistance to plastic indentation and is a key surface property influencing finishing, scratch resistance, and potential antagonist wear [97]. The alternative hypothesis (H_a) was accepted as air abrasion with 50-μm Al_2O_3 or 100-μm glass microbeads significantly altered the SH of high-translucent zirconia under thermocycling. APA-treated surfaces exceeded untreated zirconia and were within ranges reported for contemporary 5Y-PSZ/ultra-translucent zirconia [27,83,98,99]. Several studies report similarly high absolute hardness for zirconia and relative stability with aging

 doi:10.20944/preprints202510.0378.v1

[27,100]. De Araújo-Júnior et al. found 5Y-PSZ hardness to be essentially unchanged after autoclave/hydrothermal aging, suggesting intrinsic hardness is robust for modern yttria-stabilized zirconia [27]. Dejak et al. highlighted that conventional and transparent zirconia ceramics are substantially harder than enamel and often exhibit favorable, low-friction surfaces after polishing [100].

However, the near doubling of surface hardness after 50 μm Al_2O_3 APA contrasts with Yoo et al., who reported no significant change [30]. Differences may arise from APA parameters (particle type/size, pressure, time, distance, incidence angle), manufacturing route (milled vs additively made), indentation load, dwell time, or measurement of surface-localized versus subsurface hardness. Thermocycling also affects surface hardness variably. Mavriqi and Traini reported that some aging procedures can increase surface hardness, while others show little change [26]. This highlights the influence of LTD/phase transformation, surface flaws, and measurement protocols. Definitive conclusions regarding thermocycling effects on surface hardness cannot be drawn because this parameter was not explored in this study.

Clinically, zirconia hardness alone does not dictate antagonist tooth wear. Highly polished zirconia produces less enamel wear than glazed or rough surfaces. While APA increased surface hardness, it also increased surface roughness, as confirmed by stereomicroscopy and digital microscopy (Figure 4 and 5). Roughness, not hardness, is the principal driver of antagonist abrasion [87,101,102]. Effective polishing post-APA can restore a mirror finish, enabling higher hardness to confer better scratch and wear resistance. If APA leaves a rough, unpolished surface, the risk to antagonist enamel increases despite higher hardness [12,26].

The in-vitro nature of this study limits direct clinical extrapolation. Therefore, several methodological limitations and future research directions warrant careful consideration.

The manufacturer-recommended AZ zirconia primer was used. It may enhance SBS but requires strict adherence to the application protocol [74,82]. Dual-cure resin cement ResiCem, containing MDP-like phosphate monomers and fillers, can provide higher bond strength, translucency, and durable adhesion to zirconia [75]. Independent studies report superior bond strengths for ResiCem compared with self-cure cements alone, justifying its selection [96]. Using a single cement/primer and only two APA protocols limits conclusions regarding adhesive chemistry or the full APA parameter space (particle size, pressure, time, distance, incidence angle) on SBS, SH, and surface roughness [20,63,86]. Future work could expand the experimental matrix to include multiple cements and primers and systematically explore APA variables to define safe and effective protocols for cubic containing zirconia.

Although thermocycling mimics oral thermal stress, it cannot reproduce complex mechanical fatigue and multi-directional masticatory forces, which may produce different degradation patterns in adhesive interfaces [81,90]. The specific influence of thermocycling on SBS and SH under different APA protocols was not assessed in this study and warrants further study.

A macro-shear design was used for SBS testing because it is simpler and widely reported [58,103]. While tensile tests better reflect ‘true’ adhesive strength [82], the specimen geometry, bonding area, and loading protocols were standardized in this study. However, macro-shear bond strength testing concentrates load at a point and generates non-uniform stress fields, potentially overestimating bond performance compared with micro-shear or micro-tensile methods [82].

For SH estimation, Vickers microhardness was chosen for its ability to detect subtle surface changes from APA, offering superior spatial resolution compared with conventional microhardness [68,82]. APA produced statistically significant increases in surface hardness after thermocycling, demonstrating the method’s sensitivity to particle type and size. Limitations include sensitivity to surface roughness, operator variability, and focus on surface rather than bulk properties, with potential microcrack induction in brittle ceramics [80,104]. Multiple indents were averaged, but complementary bulk and surface analyses remain necessary for clinical interpretation. Micro-mechanical testing and finite-element modelling could further evaluate stress distributions under multi-directional loading [82].

 doi:10.20944/preprints202510.0378.v1

Comprehensive characterization of surface damage or phase transformation (e.g., X-ray diffraction, scanning electron microscopy coupled with energy dispersive X-ray spectroscopy, micro-computed tomography, nanoindentation mapping) was not performed. This limits interpretation of whether SH changes reflect beneficial surface hardening or deleterious subsurface flaws [81,105]. Future studies should integrate these analyses alongside bulk mechanical testing (flexural strength, fracture toughness) and antagonist wear measurements.

Small subgroup sizes (n = 5) reduce statistical power and make reliability analyses such as Weibull modulus imprecise. While Weibull parameters can be computed, estimates have high uncertainty and should be interpreted cautiously. Increasing sample sizes (≥20–30 per subgroup) permits robust analyses and uncertainty reporting via bootstrap or Bayesian intervals [106].

Material specificity further limits generalizability. Zirconia formulations vary in grain structure, phase composition, and mechanical properties; surface treatment effects observed here may not apply to other 5Y-PSZ or graded zirconia [27,60,63,66,82,83,98,99]. Translation of laboratory findings into prospective clinical trials is necessary to verify long-term retention and structural durability before issuing definitive clinical recommendations.

5. Conclusions

Within the limitations of this study, the following conclusions were obtained:

1. Airborne particle abrasion did not improve the shear bond strength, and all failure modes between the dual-cure resin cement and high-translucent zirconia were adhesive, indicating a limited benefit for resin bonding.
2. Airborne particle abrasion improves the surface hardness of high-translucent zirconia, particularly with 50 μm Al_2O_3 producing the greatest effect.

Despite existing challenges, high-translucent zirconia, with its continually evolving esthetic and mechanical properties, remains a highly versatile material in restorative dentistry and prosthodontics. Advances in surface treatments are expected to further improve its surface hardness and bond durability, thereby expanding its clinical applications.

Supplementary Materials: Not applicable.

Author Contributions: Conceptualization; methodology; software; validation; formal analysis; investigation; resources; data curation; writing—original draft preparation; writing—review and editing; visualization; supervision; project administration; funding acquisition; R.M.A. The author has read and agreed to the published version of the manuscript.

Funding: This research received no external funding.

Institutional Review Board Statement: Not applicable.

Informed Consent Statement: Not applicable.

Data Availability Statement: The raw data supporting the conclusions of this article will be made available by the author on request.

Acknowledgments: Nil.

Conflicts of Interest: The author declares no conflicts of interest. The funders had no role in the design of the study; in the collection, analyses, or interpretation of data; in the writing of the manuscript; or in the decision to publish the results.

Abbreviations

The following abbreviations are used in this manuscript:

ZrO2	Zirconium Oxide
CAD-CAM	Computer-Aided Design and Computer-Aided Manufacturing
Y_2O_3	Yttrium Oxide

 doi:10.20944/preprints202510.0378.v1

3Y-TZP	3 mol% Yttria-stabilized Tetragonal Zirconia Polycrystal
Al_2O_3	Aluminium Oxide
4Y-PSZ	4 mol% Yttria-Partially Stabilized Zirconia
5Y-PSZ	5 mol% Yttria-Partially Stabilized Zirconia
LTD	Low Temperature Degradation
APA	Airborne Particle Abrasion
ZSAT	Zirconia Surface Architecturing Technique
10-MDP	10-Methacryloyloxydecyl Dihydrogen Phosphate
SBS	Shear Bond Strength
SH	Surface Hardness
Ni-Cr	Nickel-Chromium
H_0	Null hypothesis
H_a	Alternative hypothesis
UDMA	Urethane Dimethacrylate
TEGDMA	Triethylene Glycol Dimethacrylate
AET	Acryloxyethyltrimellitic Acid
HEMA	Hydroxyethyl Methacrylate
MHPA	Methacryloyloxyhexyl Phosphonoacetate
SD	Standard deviation
P	Probability
VHN	Vickers Hardness Number
t→m	tetragonal→monoclinic

References

1. Hussien, Z.Y.; Moften, A.Q.; Abdulrehman, M.A. Review of zirconia (ZrO_2) biomedical applications: Advanced manufacturing techniques and materials properties. Revue des Composites et des Matériaux Avancés 2025, 35, 345–353.
2. Bapat, R.A.; Yang, H.J.; Chaubal, T.V.; Dharmadhikari, S.; Abdulla, A.M.; Arora, S.; Rawal, S.; Kesharwani, P. Review on synthesis, properties and multifarious therapeutic applications of nanostructured zirconia in dentistry. RSC Adv. 2022, 12, 12773–12793.
3. Sudarshanan, A.; Kurian, B.P.; Joseph, A.M. CAD–CAM technology and its application in prosthodontics: An overview. Malanadu Dental Journal 2018, 7(3), 226–233.
4. Joseph, A.M.; Aldhuwayhi, S.D.; Mustafa, M.Z.; Deeban, Y.; Thakare, A.A.; Joseph, A. Fingernail form as a post-extraction guide for selecting the maxillary central incisor tooth form in the Saudi Arabian population: A novel application of CAD software. Niger. J. Clin. Pract. 2023, 26(8), 1157–1164.
5. Karapetyan, H. The use of zirconium dioxide in dentistry and oral implantology: Narrative review. Bull. Stomatol. Maxillofac. Surg. 2025, 21(2), 188–199.
6. Nistor, L.; Grădinaru, M.; Rîcă, R.; Mărășescu, P.; Stan, M.; Manolea, H.; Ionescu, A.; Moraru, I. Zirconia Use in Dentistry—Manufacturing and Properties. Curr. Health Sci. J. 2019, 45(1), 28–35.
7. Khan, A.S.; Musani, S.; Madanshetty, P.; Shaikh, T.; Shaikh, M.; Lal, Q. A Study of the Antagonist Tooth Wear, Hardness, and Fracture Toughness of Three Different Generations of Zirconia. World J. Dent. 2023, 14(8), 688–695.
8. Miura, S.; Fujita, T.; Fujisawa, M. Zirconia in fixed prosthodontics: A review of the literature. Odontology 2025, 113(2), 466–487.
9. Cuzic, C.; Rominu, M.; Pricop, A.; Urechescu, H.; Pricop, M.O.; Rotar, R.; Cuzic, O.S.; Sinescu, C.; Jivanescu, A. Clinician's Guide to Material Selection for All-Ceramics in Modern Digital Dentistry. Materials 2025, 18(10), 2235.
10. Mao, Z.; Schmidt, F.; Beuer, F.; Yassine, J.; Hey, J.; Prause, E. Effect of surface treatment strategies on bond strength of additively and subtractively manufactured hybrid materials for permanent crowns. Clin. Oral Investig. 2024, 28(7), 371.
11. Al-Amari, A.S.; Saleh, M.S.; Albadah, A.A.; Almousa, A.A.; Mahjoub, W.K.; Al-Otaibi, R.M.; Alanazi, E.M.; Alshammari, A.K.; Malki, A.T.; Alghelaiqah, K.F.; Akbar, L.F. A Comprehensive Review of Techniques for Enhancing Zirconia Bond Strength: Current Approaches and Emerging Innovations. Cureus 2024, 16(10), e70893.

 doi:10.20944/preprints202510.0378.v1

12. Ban, S. Classification and Properties of Dental Zirconia as Implant Fixtures and Superstructures. Materials 2021, 14(17), 4879.
13. Toksoy, D.; Önöral, Ö. Optical Behavior of Zirconia Generations. Cyprus J. Med. Sci. 2024, 9(6), 380–389.
14. Stawarczyk, B.; Keul, C.; Eichberger, M.; Figge, D.; Edelhoff, D.; Lümkemann, N. Three Generations of Zirconia: From Veneered to Monolithic. Part I. Quintessence Int. 2017, 48(5), 369–380.
15. Pizzolatto, G.; Borba, M. Optical Properties of New Zirconia-Based Dental Ceramics: Literature Review. Cerâmica 2021, 67(383), 338–343.
16. Zhang, F.; Van Meerbeek, B.; Vleugels, J. Importance of Tetragonal Phase in High-Translucent Partially Stabilized Zirconia for Dental Restorations. Dent. Mater. 2020, 36(4), 491–500.
17. Jerman, E.; Lümkemann, N.; Eichberger, M.; Zoller, C.; Nothelfer, S.; Kienle, A.; Stawarczyk, B. Evaluation of translucency, Martens's hardness, biaxial flexural strength and fracture toughness of 3Y-TZP, 4Y-TZP and 5Y-TZP materials. Dent. Mater. 2021, 37(2), 212–222.
18. Manziuc, M.-M.; Gasparik, C.; Negucioiu, M.; Constantiniuc, M.; Burde, A.; Vlas, I.; Dudea, D. Optical properties of translucent zirconia: A review of the literature. EuroBiotech J. 2019, 3(1), 45–51.
19. Yousry, M.; Hammad, I.; Halawani, M.E.; Aboushelib, M. Translucency of recent zirconia materials and material-related variables affecting their translucency: A systematic review and meta-analysis. BMC Oral Health 2024, 24(1), 309.
20. Sales, A.; Rodrigues, S.J.; Mahesh, M.; Ginjupalli, K.; Shetty, T.; Pai, U.Y.; Saldanha, S.; Hegde, P.; Mukherjee, S.; Kamath, V.; Bajantri, P.; Srikant, N.; Kotian, R. Effect of different surface treatments on the micro-shear bond strength and surface characteristics of zirconia: An in vitro study. Int. J. Dent. 2022, 2022, 1546802.
21. Pieniak, D.; Walczak, A.; Walczak, M.; Przystupa, K.; Niewczas, A.M. Hardness and wear resistance of dental biomedical nanomaterials in a humid environment with non-stationary temperatures. Materials 2020, 13(5), 1255.
22. Cesar, P.F.; Miranda, R.B.P.; Santos, K.F.; Scherrer, S.S.; Zhang, Y. Recent advances in dental zirconia: 15 years of material and processing evolution. Dent. Mater. 2024, 40(5), 824–836.
23. Wang, L.; Wang, K.; Hao, Z.; Dou, R.; Zhu, F.; Gao, Y. Fracture toughness and subcritical crack growth analysis of high-translucent zirconia prepared by stereolithography-based additive manufacturing. J. Mech. Behav. Biomed. Mater. 2025, 164, 106917.
24. Li, Q.; Yang, Y.; Chen, K.; Jiang, Y.; Swain, M.V.; Yao, M.; He, Y.; Liang, Y.; Jian, Y.; Zhao, K. Effect of low-temperature degradation on the fatigue performance of dental strength-gradient multilayered zirconia restorations. J. Dent. 2024, 142, 104866.
25. Park, M.G. Effect of low-temperature degradation treatment on hardness, color, and translucency of single layers of multilayered zirconia. J. Prosthet. Dent. 2025, 133(1), 258–263.
26. Mavriqi, L.; Traini, T. Mechanical properties of translucent zirconia: An in vitro study. Prosthesis 2023, 5, 48–59.
27. de Araujo-Junior, E.N.S.; Bergamo, E.T.P.; Bastos, T.M.C.; Benalcázar Jalkh, E.B.; Lopes, A.C.O.; Monteiro, K.N.; Cesar, P.F.; Tognolo, F.C.; Migliati, R.; Tanaka, R.; Bonfante, E.A. Ultra-translucent zirconia processing and aging effect on microstructural, optical, and mechanical properties. Dent. Mater. 2022, 38(4), 587–600.
28. Mohamed, S.G.A.; Hussein, H.G.A.; Mohamed, G.A.; Ibrahim, S.R.M. Different Zirconia Surface Treatments: Strategies to Enhance Adhesion in Zirconia-Based Dental Restorations. J. Pharm. Bioallied Sci. 2025, 17, 45–49.
29. Scaminaci Russo, D.; Cinelli, F.; Sarti, C.; Giachetti, L. Adhesion to Zirconia: A Systematic Review of Current Conditioning Methods and Bonding Materials. Dent. J. 2019, 7, 74.
30. Yoo, L.G.; Pang, N.S.; Kim, S.H.; Jung, B.Y. Mechanical properties of additively manufactured zirconia with alumina air abrasion surface treatment. Sci. Rep. 2023, 13, 9153.
31. Nagaoka, N.; Yoshihara, K.; Tamada, Y.; Yoshida, Y.; Van Meerbeek, B. Ultrastructure and bonding properties of tribochemical silica-coated zirconia. Dent. Mater. J. 2019, 38(1), 107–113.

 doi:10.20944/preprints202510.0378.v1

32. Yahyazadehfar, N.; Azimi Zavaree, M.; Shayegh, S.S.; Yahyazadehfar, M.; Hooshmand, T.; Hakimaneh, S.M.R. Effect of different surface treatments on surface roughness, phase transformation, and biaxial flexural strength of dental zirconia. J. Dent. Res. Dent. Clin. Dent. Prospects 2021, 15(3), 210–218.
33. Lee, J.Y.; Jang, G.W.; Park, I.I.; Heo, Y.R.; Son, M.K. The effects of surface grinding and polishing on the phase transformation and flexural strength of zirconia. J. Adv. Prosthodont. 2019, 11(1), 1–6.
34. Abdullah, H.; Abdulsamee, N.; Farouk, H.; Saba, D.A. Effect of Er:YAG laser surface treatment on surface properties and shear-bond strength of resin-cement to three translucent zirconia: An in vitro study. Discov. Mater. 2024, 4, 35.
35. Bitencourt, S.B.; Ferreira, L.C.; Mazza, L.C.; Dos Santos, D.M.; Pesqueira, A.A.; Theodoro, L.H. Effect of laser irradiation on bond strength between zirconia and resin cement or veneer ceramic: A systematic review and meta-analysis. J. Indian Prosthodont. Soc. 2021, 21(2), 125–137.
36. Ergun Kunt, G.; Duran, I. Effects of laser treatments on surface roughness of zirconium oxide ceramics. BMC Oral Health 2018, 18(1), 222.
37. Çakırbay Tanış, M.; Akay, C.; Şen, M. Effect of selective infiltration etching on the bond strength between zirconia and resin luting agents. J. Esthet. Restor. Dent. 2019, 31(3), 257–262.
38. Kaimal, A.; Ramdev, P.; Shruthi, C.S. Evaluation of effect of zirconia surface treatment, using plasma of argon and silane, on the shear bond strength of two composite resin cements. J. Clin. Diagn. Res. 2017, 11(8), ZC39–ZC43.
39. Tabari, K.; Hosseinpour, S.; Mohammad-Rahimi, H. The impact of plasma treatment of Cercon® zirconia ceramics on adhesion to resin composite cements and surface properties. J. Lasers Med. Sci. 2017, 8 (Suppl. 1), S56–S61.
40. Skienhe, H.; Abdou, A.; Matinlinna, J.P.; Ferrari, M.; Salameh, Z. Effect of low-fusing porcelain glaze as zirconia surface treatment on the adhesion of resin cement. J. Clin. Exp. Dent. 2025, 17(4), e407–e415.
41. Malgaj, T.; Mirt, T.; Kocjan, A.; Jevnikar, P. The Influence of Nanostructured Alumina Coating on Bonding and Optical Properties of Translucent Zirconia Ceramics: In Vitro Evaluation. Coatings 2021, 11, 1126.
42. Külünk, T.; Külünk, Ş.; Baba, S.; Oztürk, Ö.; Danişman, Ş.; Savaş, S. The effect of alumina and aluminium nitride coating by reactive magnetron sputtering on the resin bond strength to zirconia core. J. Adv. Prosthodont. 2013, 5(4), 382–387.
43. Lv, P.; Yang, X.; Jiang, T. Influence of hot-etching surface treatment on zirconia/resin shear bond strength. Materials 2015, 8 (12), 8087–8096.
44. Liang, Z.; Liu, Y.; Jiang, Y.; Liu, P.; Zhang, Y.; Meng, F.; Liu, M.; Cui, Z.; Ma, J.; Chen, J. Effect of hot etching with HF on the surface topography and bond strength of zirconia. Front. Mater. 2022, 9, 1008704.
45. Gołasz, P.; Kołkowska, A.; Zieliński, R.; Simka, W. Zirconium Surface Treatment via Chemical Etching. Materials 2023, 16, 7404.
46. Nojedehian, H.; Moezzizadeh, M.; Abdollahi, N.; Soltaninejad, F.; Valizadeh Haghi, H. The effect of bioglass coating on microshear bond strength of resin cement to zirconia. Front. Dent. 2024, 21, 6.
47. Liu, D.; Pow, E.H.N.; Tsoi, J.K.; Matinlinna, J.P. Evaluation of four surface coating treatments for resin to zirconia bonding. J. Mech. Behav. Biomed. Mater. 2014, 32, 300–309.
48. Her, S.B.; Kim, K.H.; Park, S.E.; Park, E.J. The effect of zirconia surface architecturing technique on the zirconia/veneer interfacial bond strength. J. Adv. Prosthodont. 2018, 10(4), 259–264.
49. Wongkamhaeng, K.; Poomparnich, K.; Chitkraisorn, T.; Boonpitak, K.; Tosiriwatanapong, T. Effect of combining different 10-MDP-containing primers and cement systems on shear bond strength between resin cement and zirconia. BMC Oral Health 2025, 25, 206.
50. Jalaj, V.; Kamath, V.; Pai, U.; Natarajan, S.; S, S.; Gupta, A. Effect of sandblasting and MDP-based primer application on the surface topography and shear bond strength of zirconia: An in vitro study. F1000Res. 2025, 14, 642.
51. Shen, D.; Wang, H.; Shi, Y.; Su, Z.; Hannig, M.; Fu, B. The Effect of Surface Treatments on Zirconia Bond Strength and Durability. J. Funct. Biomater. 2023, 14, 89.
52. Ishii, R.; Tsujimoto, A.; Takamizawa, T.; Tsubota, K.; Suzuki, T.; Shimamura, Y.; Miyazaki, M. Influence of surface treatment of contaminated zirconia on surface free energy and resin cement bonding. Dent. Mater. J. 2015, 34(1), 91–97.

 doi:10.20944/preprints202510.0378.v1

53. Feitosa, S.A.; Lima, N.B.; Yoshito, W.K.; Campos, F.; Bottino, M.A.; Valandro, L.F.; Bottino, M.C. Bonding strategies to full-contour zirconia: Zirconia pretreatment with piranha solution, glaze and airborne-particle abrasion. Int. J. Adhes. Adhes. 2017, 77, 151–156.
54. Kim, S.-H.; Cho, S.-C.; Lee, M.-H.; Kim, H.-J.; Oh, N.-S. Effect of 9% Hydrofluoric Acid Gel Hot-Etching Surface Treatment on Shear Bond Strength of Resin Cements to Zirconia Ceramics. Medicina 2022, 58, 1469.
55. Liu, X.; Wang, H.; Yu, S.; Zhao, Q.; Shi, Z.; Cui, Z.; Zhu, S. Construction of a silicate-based epitaxial transition film on a zirconia ceramic surface to improve the bonding quality of zirconia restorations. RSC Adv. 2020, 10, 32476–32484.
56. Batista, A.; Palacios, N.; Jiménez, O.R. Zirconia Cementation: A Systematic Review of the Most Currently Used Protocols. Open Dent. J. 2024, 18, e18742106300869.
57. Li, X.; Liang, S.; Inokoshi, M.; Zhao, S.; Hong, G.; Yao, C.; Huang, C. Different surface treatments and adhesive monomers for zirconia-resin bonds: A systematic review and network meta-analysis. Jpn. Dent. Sci. Rev. 2024, 60, 175–189.
58. Rigos, A.E.; Sarafidou, K.; Kontonasaki, E. Zirconia bond strength durability following artificial aging: A systematic review and meta-analysis of in vitro studies. Jpn. Dent. Sci. Rev. 2023, 59, 138–159.
59. Alves, M.F.R.P.; dos Santos, C.; Elias, C.N.; Amarante, J.E.V.; Ribeiro, S. Comparison between different fracture toughness techniques in zirconia dental ceramics. J. Biomed. Mater. Res. B Appl. Biomater. 2023, 111, 103–116.
60. Alrabeah, G.; Al-Sowygh, A.H.; Almarshedy, S. Use of Ultra-Translucent Monolithic Zirconia as Esthetic Dental Restorative Material: A Narrative Review. Ceramics 2024, 7, 264–275.
61. Blatz, M.B.; Alvarez, M.; Sawyer, K.; Brindis, M. How to Bond Zirconia: The APC Concept. Compend. Contin. Educ. Dent. 2016, 37, 611–617.
62. Alshali, R. Z.; Alqahtani, M. A.; Alturki, B. N.; Algizani, L. I.; Batarfi, A. O.; Alshamrani, Z. K.; Faden, R. M.; Bukhary, D. M.; Altassan, M. M. Effect of air-particle abrasion and methacryloyloxydecyl phosphate primer on fracture load of thin zirconia crowns: An in vitro study. Front. Dent. Med. 2024, 5, 1501909.
63. Almutairi, R.; Elhejazi, A.; Alnahedh, H.; Maawadh, A. Effects of different airborne particle abrasion protocols on the surface roughness and shear bonding strength of high/ultra-translucent zirconia to resin cement. Ceramics-Silikáty 2021, 65, 401–409.
64. Flores-Ferreyra, B.I.; Moyaho-Bernal, M.L.A.; Chavarría-Lizárraga, H.N.; Castro-Ramos, J.; Franco-Romero, G.; Velázquez-Enríquez, U.; Flores-Ledesma, A.; Reyes-Cervantes, E.; Ley-García, A.K.; Velasco-León, E.D.C.; Carrasco-Gutiérrez, R.G. Surface treatment, chemical characterization, and debonding crack initiation strength for veneering dental ceramics on Ni-Cr alloys. Materials 2025, 18, 3822.
65. Nobuaki, A.; Keiichi, Y.; Takashi, S. Effects of air abrasion with alumina or glass beads on surface characteristics of CAD/CAM composite materials and the bond strength of resin cements. J. Appl. Oral Sci. 2015, 23, 629–636.
66. AlMutairi, R.; AlNahedh, H.; Maawadh, A.; Elhejazi, A. Effects of Different Air Particle Abrasion Protocols on the Biaxial Flexural Strength and Fractography of High/Ultra-Translucent Zirconia. Materials 2022, 15, 244.
67. Kui, A.; Buduru, S.; Labunet, A.; Sava, S.; Pop, D.; Bara, I.; Negucioiu, M. Air Particle Abrasion in Dentistry: An Overview of Effects on Dentin Adhesion and Bond Strength. Dent. J. 2025, 13, 16.
68. Turp, V.; Sen, D.; Tuncelli, B.; Goller, G.; Özcan, M. Evaluation of air-particle abrasion of Y-TZP with different particles using microstructural analysis. Aust. Dent. J. 2013, 58, 183–191.
69. Lagodzinska, P.; Dejak, B.; Konieczny, B. The influence of alumina airborne-particle abrasion on the properties of zirconia-based dental ceramics (3Y-TZP). Coatings 2023, 13, 1691.
70. Moon, J.E.; Kim, S.H.; Lee, J.B.; Han, J.S.; Yeo, I.S.; Ha, S.R. Effects of airborne-particle abrasion protocol choice on the surface characteristics of monolithic zirconia materials and the shear bond strength of resin cement. Ceram. Int. 2016, 42, 1552–1562.
71. Shofu Dental Asia-Pacific. ZR Lucent. Available online: https://www.shofu.com.sg/product/zr-lucent/ (accessed on 3 October 2025).
72. BEGO GmbH & Co. KG. Korox 50. Available online: https://eshop.bego.com/en-en/products/den_46062 (accessed on 3 October 2025).

 doi:10.20944/preprints202510.0378.v1

73. Renfert GmbH. Rolloblast 100 µm. Available online: https://www.renfert.com/en/products/materials/dental-abrasives/rolloblast (accessed on 3 October 2025).
74. Shofu Dental Asia-Pacific. AZ Primer. Available online: https://shofu.co.in/available_products/az-primer (accessed on 3 October 2025).
75. Shofu Dental Asia-Pacific. ResiCem. Available online: https://www.shofu.com.sg/product/resicem/ (accessed on 3 October 2025).
76. Carek, A.; Dukaric, K.; Miler, H.; Marovic, D.; Tarle, Z.; Par, M. Post-Cure Development of the Degree of Conversion and Mechanical Properties of Dual-Curing Resin Cements. Polymers 2022, 14, 3649.
77. Gale, M.S.; Darvell, B.W. Thermal cycling procedures for laboratory testing of dental restorations. J. Dent. 1999, 27, 89–99.
78. Serra-Prat, J.; Cano-Batalla, J.; Cabratosa-Termes, J.; Figueras-Àlvarez, O. Adhesion of dental porcelain to cast, milled, and laser-sintered cobalt-chromium alloys: Shear bond strength and sensitivity to thermocycling. J. Prosthet. Dent. 2014, 112, 600–605.
79. Colombo, M.; Poggio, C.; Lasagna, A.; Chiesa, M.; Scribante, A. Vickers Micro-Hardness of New Restorative CAD/CAM Dental Materials: Evaluation and Comparison after Exposure to Acidic Drink. Materials 2019, 12, 1246.
80. Kosmac, T.; Oblak, C.; Jevnikar, P.; Funduk, N.; Marion, L. The effect of surface grinding and sandblasting on flexural strength and reliability of Y-TZP zirconia ceramic. Dent. Mater. 1999, 15, 426–433.
81. Al-Shehri, E.Z.; Al-Zain, A.O.; Sabrah, A.H.; Al-Angari, S.S.; Al Dehailan, L.; Eckert, G.J.; Özcan, M.; Platt, J.A.; Bottino, M.C. Effects of air-abrasion pressure on the resin bond strength to zirconia: A combined cyclic loading and thermocycling aging study. Restor. Dent. Endod. 2017, 42, 206–215.
82. Tzanakakis, E.; Tzoutzas, I.; Koidis, P. Is there a potential for durable adhesion to zirconia restorations? A systematic review. J. Prosthet. Dent. 2016, 115, 7–18.
83. Mao, L.; Kaizer, M.R.; Zhao, M.; Guo, B.; Song, Y.F.; Zhang, Y. Graded ultra-translucent zirconia (5Y-PSZ) for strength and functionalities. J. Dent. Res. 2018, 97, 1222–1228.
84. McLaren, E.A.; Lawson, N.; Choi, J.; Kang, J.; Trujillo, C. New high-translucent cubic-phase-containing zirconia: Clinical and laboratory considerations and the effect of air abrasion on strength. Compend. Contin. Educ. Dent. 2017, 38, e13–e16.
85. Michida, S.M. de A.; Kimpara, E.T.; dos Santos, C.; Souza, R.O.A.; Bottino, M.A.; Özcan, M. Effect of air-abrasion regimens and fine diamond bur grinding on flexural strength, Weibull modulus and phase transformation of zirconium dioxide. J. Appl. Biomater. Funct. Mater. 2015, 13, 266–273.
86. Mehari, K.; Parke, A.S.; Gallardo, F.F.; Vandewalle, K.S. Assessing the Effects of Air Abrasion with Aluminum Oxide or Glass Beads to Zirconia on the Bond Strength of Cement. J. Contemp. Dent. Pract. 2020, 21, 713–717.
87. Alrabeah, G.; Alomar, S.; Almutairi, A.; Alali, H.; ArRejaie, A. Analysis of the effect of thermocycling on bonding cements to zirconia. Saudi Dent. J. 2023, 35, 734–740.
88. Li, Z.; Yan, X.; Toufani, N.; Sano, H.; Fu, J. Curing modes affect micro-tensile bond strength and durability of dual curing resin cements to dentin. Front. Bioeng. Biotechnol. 2025, 12, 1511099.
89. Samran, A.; Al-Ammari, A.; El Bahra, S.; Halboub, E.; Wille, S.; Kern, M. Bond strength durability of self-adhesive resin cements to zirconia ceramic: An in vitro study. J. Prosthet. Dent. 2019, 121, 477–484.
90. Cho, J.H.; Kim, S.J.; Shim, J.S.; Lee, K.W. Effect of zirconia surface treatment using nitric acid-hydrofluoric acid on the shear bond strengths of resin cements. J. Adv. Prosthodont. 2017, 9, 77–84.
91. Amaral, M.; Belli, R.; Cesar, P.F.; Valandro, L.F.; Petschelt, A.; Lohbauer, U. The potential of novel primers and universal adhesives to bond to zirconia. J. Dent. 2014, 42, 90–98.
92. Alammar, A.; Blatz, M.B. The resin bond to high-translucent zirconia: A systematic review. J. Esthet. Restor. Dent. 2022, 34, 117–135.
93. Kui, A.; Manziuc, M.; Petruțiu, A.; Buduru, S.; Labunet, A.; Negucioiu, M.; Chisnoiu, A. Translucent zirconia in fixed prosthodontics—An integrative overview. Biomedicines 2023, 11, 3116.
94. Abdou, A.; Hussein, N.; Kusumasari, C.; et al. Alumina and glass-bead blasting effect on bond strength of zirconia using 10-methacryloyloxydecyl dihydrogen phosphate (MDP) containing self-adhesive resin cement and primers. Sci. Rep. 2023, 13, 19127.

 doi:10.20944/preprints202510.0378.v1

95. Al-Amari, A.S.; Saleh, M.S.; Albadah, A.A.; Almousa, A.A.; Mahjoub, W.K.; Al-Otaibi, R.M.; Alanazi, E.M.; Alshammari, A.K.; Malki, A.T.; Alghelaiqah, K.F.; Akbar, L.F. A comprehensive review of techniques for enhancing zirconia bond strength: Current approaches and emerging innovations. Cureus 2024, 16, e70893.
96. Li, X.; Liang, S.; Li, J.; Tang, W.; Yu, M.; Ahmed, M.H.; Liang, S.; Zhang, F.; Inokoshi, M.; Yao, C.; Huang, C. Influence of surface treatments on highly translucent zirconia: Mechanical, optical properties and bonding performance. J. Dent. 2025, 154, 105580.
97. Joseph, A.M.; Joseph, S.; Mathew, N.; Koshy, A.T.; Jayalakshmi, N.L.; Mathew, V. Effect of incorporation of nanoclay on the properties of heat cure denture base material: An in vitro study. Contemp. Clin. Dent. 2019, 10, 658–663.
98. Shofu Dental Europe. ZR Lucent Supra. Available online: https://www.shofu-dental.fr/en/produkt/shofu-disk-zr-lucent-supra-en (accessed on 3 October 2025).
99. Nakai, H.; Inokoshi, M.; Liu, H.; Uo, M.; Kanazawa, M. Evaluation of extra-high translucent dental zirconia: Translucency, crystalline phase, mechanical properties, and microstructures. J. Funct. Biomater. 2025, 16, 13.
100. Dejak, B.D.; Langot, C.; Krasowski, M.; Klich, M. Evaluation of hardness and wear of conventional and transparent zirconia ceramics, feldspathic ceramic, glaze, and enamel. Materials 2024, 17, 3518.
101. Kongkiatkamon, S.; Booranasophone, K.; Tongtaksin, A.; Kiatthanakorn, V.; Rokaya, D. Comparison of fracture load of the four translucent zirconia crowns. Molecules 2021, 26, 5308.
102. Kongkiatkamon, S.; Rokaya, D.; Kengtanyakich, S.; Peampring, C. Current classification of zirconia in dentistry: An updated review. PeerJ 2023, 11, e15669.
103. Sarıkaya, I.; Hayran, Y. Adhesive bond strength of monolithic zirconia ceramic finished with various surface treatments. BMC Oral Health 2023, 23, 858.
104. Aguiar, T.C.; Saad, J.R.C.; Pinto, S.C.S.; Calixto, L.R.; Lima, D.M.; Silva, M.A.S.; et al. The effects of exposure time on the surface microhardness of three dual-cured dental resin cements. Polymers 2011, 3, 998–1005.
105. Kim, S.H.; Oh, K.C.; Moon, H.S. Effects of surface-etching systems on the shear bond strength of dual-polymerized resin cement and zirconia. Materials 2024, 17, 3096.
106. Osuchukwu, O.A.; Salihi, A.; Ibrahim, A.; Audu, A.A.; Makoyo, M.; Mohammed, S.A.; Lawal, M.Y.; Etinosa, P.O.; Isaac, I.O.; Oni, P.G.; Oginni, O.G.; Obada, D.O. Weibull analysis of ceramics and related materials: A review. Heliyon 2024, 10, e32495.